



Formation and dissipation mechanisms of AGN jets

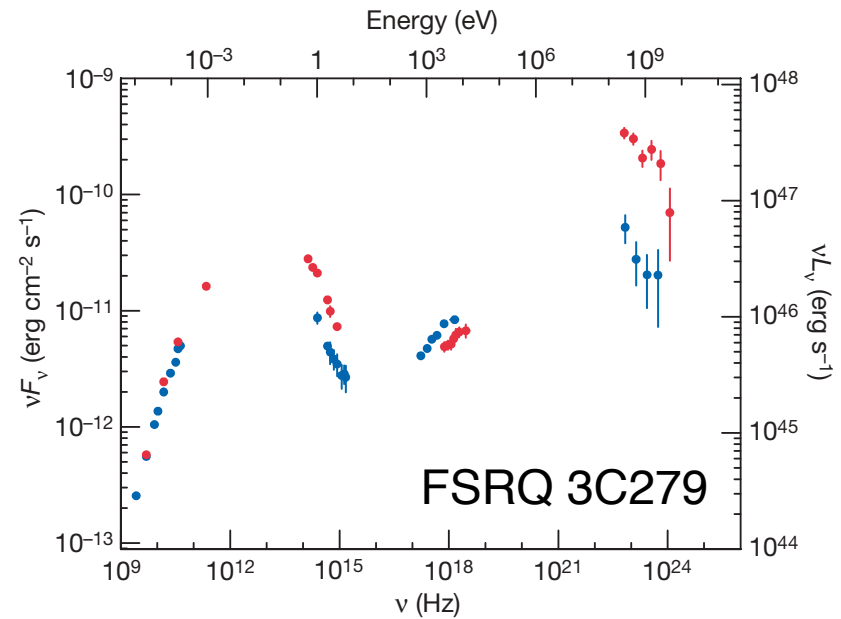
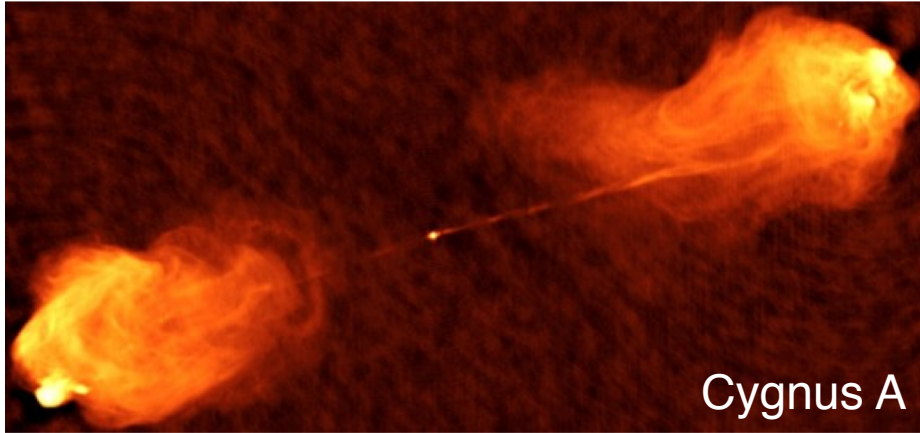
Kenji TOMA (FRIS, Tohoku U)

K. Takahashi (YITP), M. Nakamura (ASIAA), M. Kino (Kogakuin U),
T. Oghihara (Tohoku U), K. Hada (NAOJ)

Outline

- Introduction: theoretical issues on AGN jets
- Limb-brightening of M87 jet
 - Axisymmetry vs synchrotron model image
 - Width profile vs GRMHD simulation
- Mass-loading problem

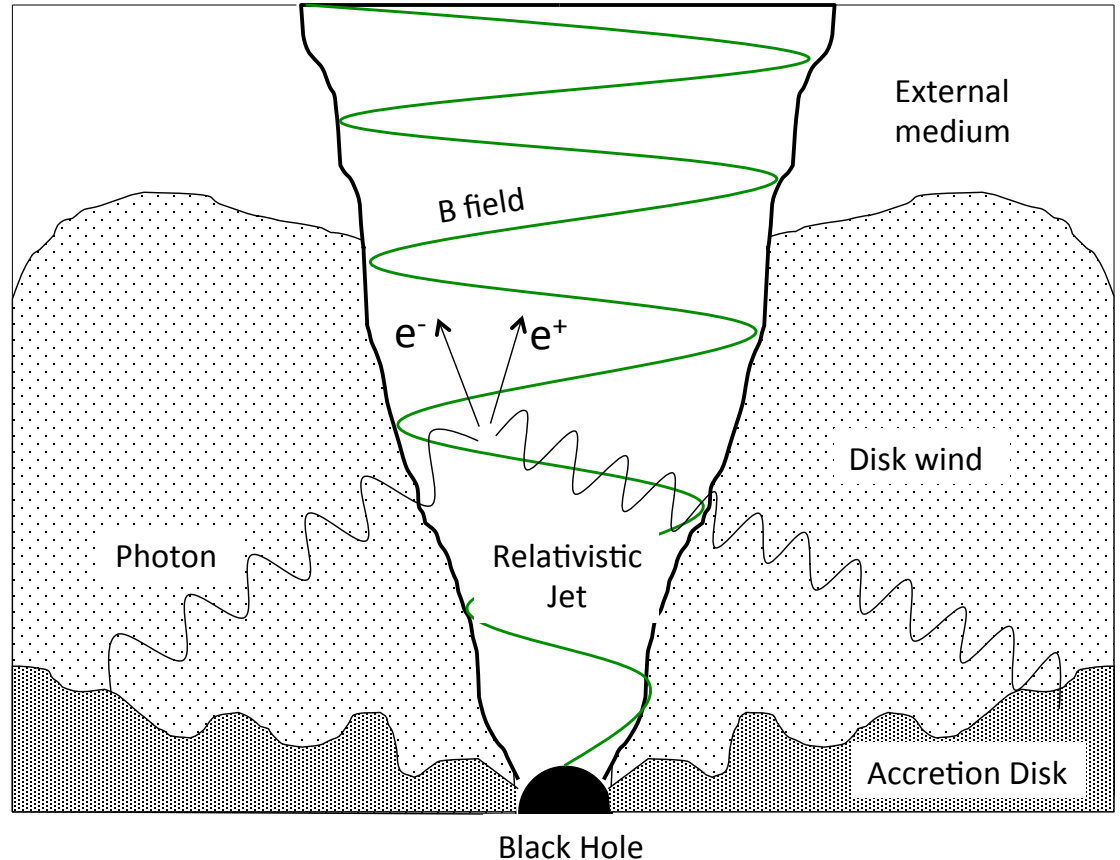
AGN jets



- Radio galaxies (mainly elliptical)
 - FR-I / FR-II
- Blazars
 - BL Lacs / Flat Spectrum Radio Quasars

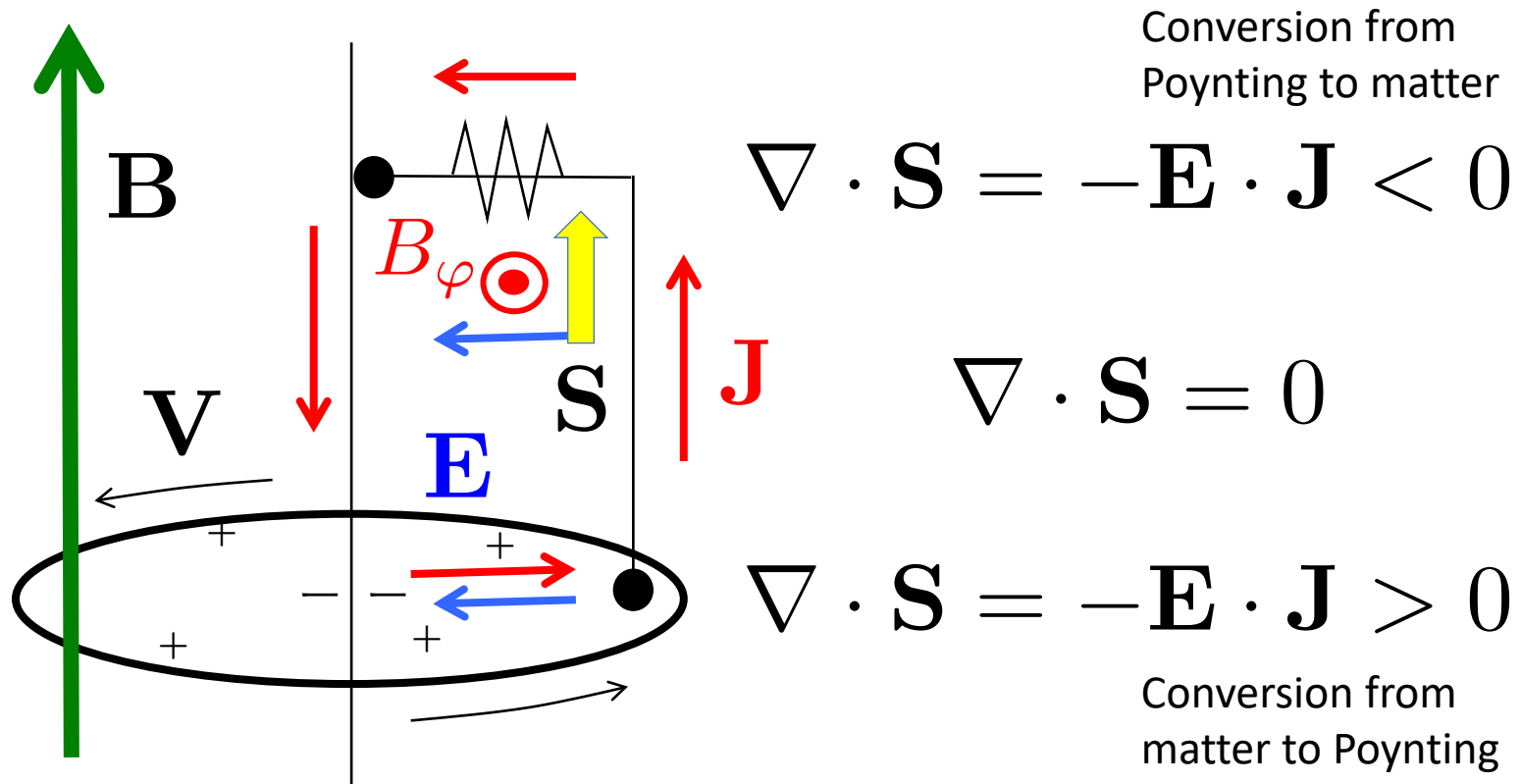
Theoretical issues

- Energy source
- Mass source
- Acceleration
- Collimation
- Stability
- Dissipation
- ...



Koide et al. 2000; Komissarov 2001; McKinney & Gammie 2004;
Barkov & Komissarov 2008; Tchekhovskoy et al. 2011; Ruiz et al.
2012; Contopoulos et al. 2013

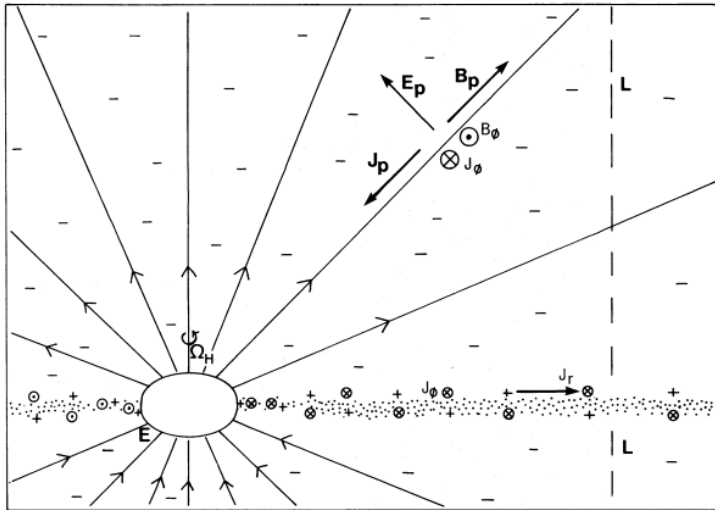
Energy source



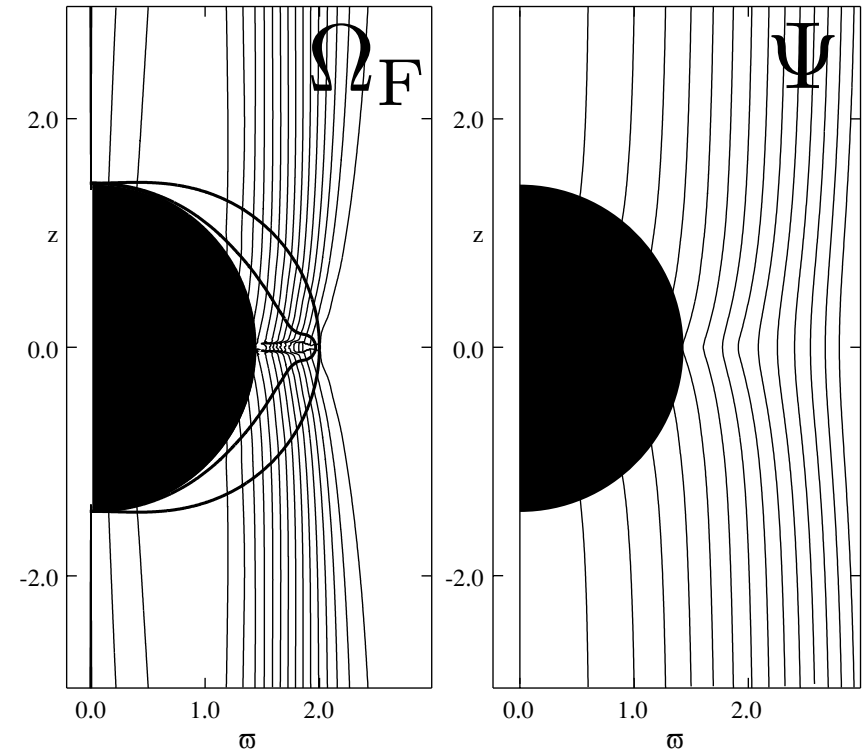
- Rotating BH or accretion disk?
- (fireball is unlikely for AGN jets)

Blandford-Znajek process

Resistive force-free simulation



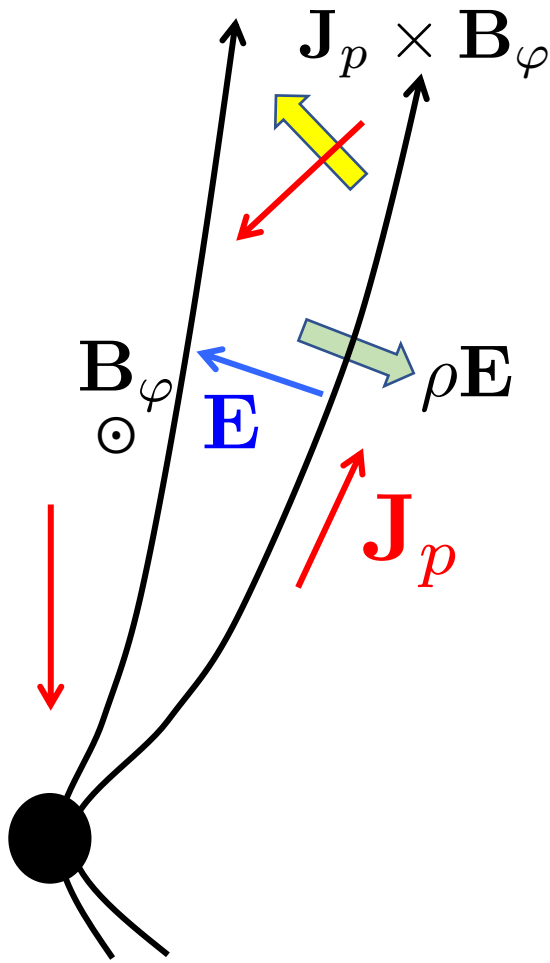
$$\mathbf{E} = -\Omega_F \mathbf{e}_\phi \times \mathbf{B}$$



Ergosphere does not allow force-free plasma with no outward Poynting flux

$$(B^2 - D^2)\alpha^2 = -B^2 f(\Omega_F, r, \theta) + \frac{1}{\alpha^2} (\Omega_F - \Omega)^2 H_\varphi^2$$

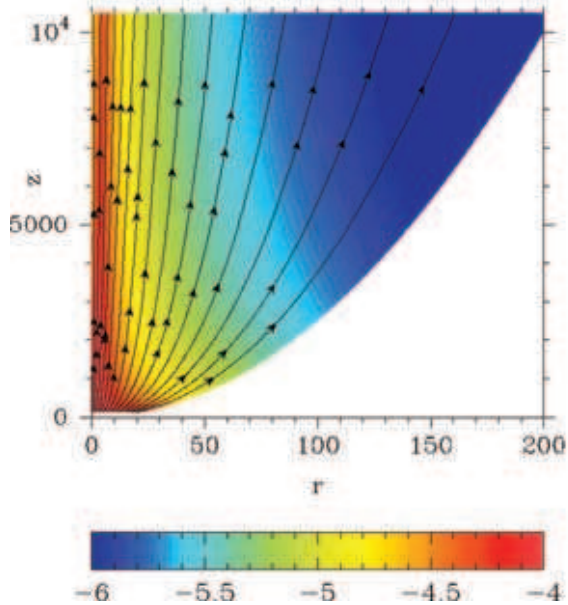
Acceleration / collimation



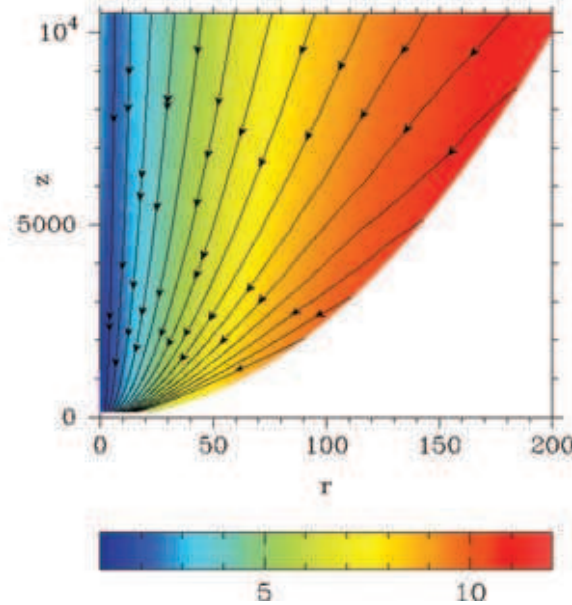
- Energy conversion from Poynting to fluid by $\mathbf{E} \cdot \mathbf{J} = (-\mathbf{V} \times \mathbf{B}) \cdot \mathbf{J} = (\mathbf{J} \times \mathbf{B}) \cdot \mathbf{V}$
- $\mathbf{J} \times \mathbf{B}$ force also collimates the flow, but $\rho \mathbf{E}$ force prevents it
 -> B_ϕ^2 stress is not effective for relativistic fluid
 -> External pressure required to collimate relativistic flow

Large-scale SRMHD simulation

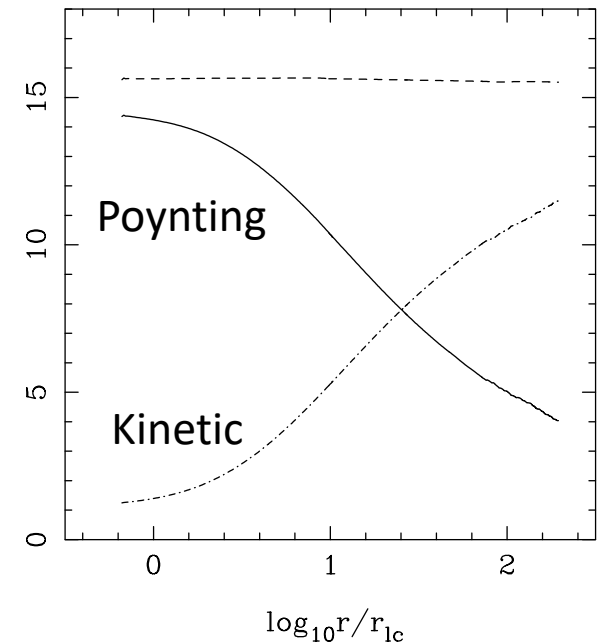
Field lines and $\Gamma\rho$



Current lines and Γ

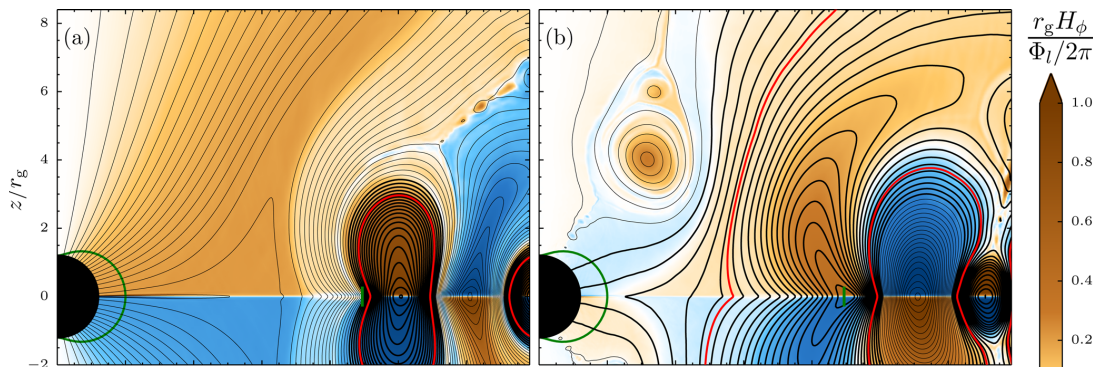
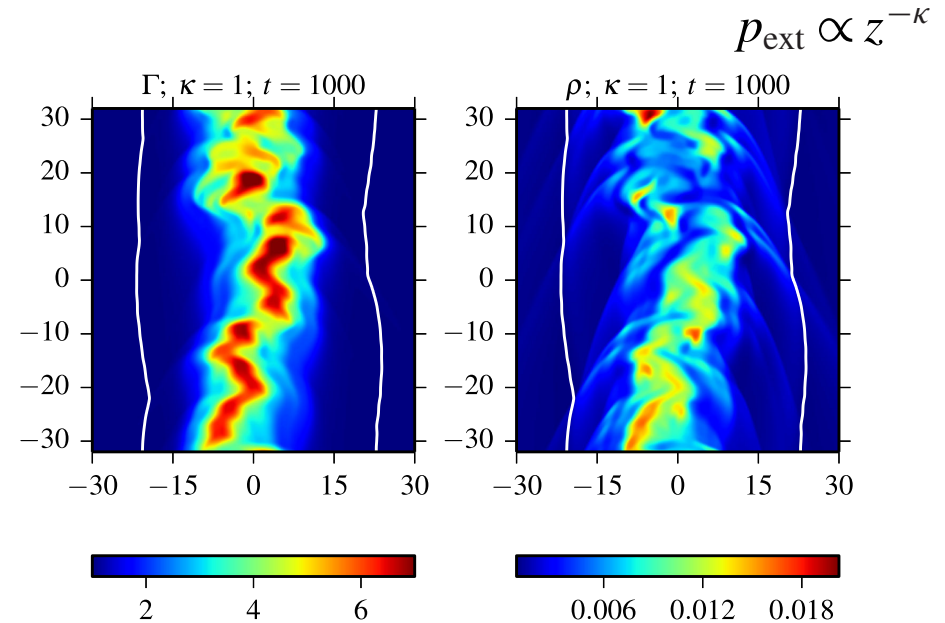
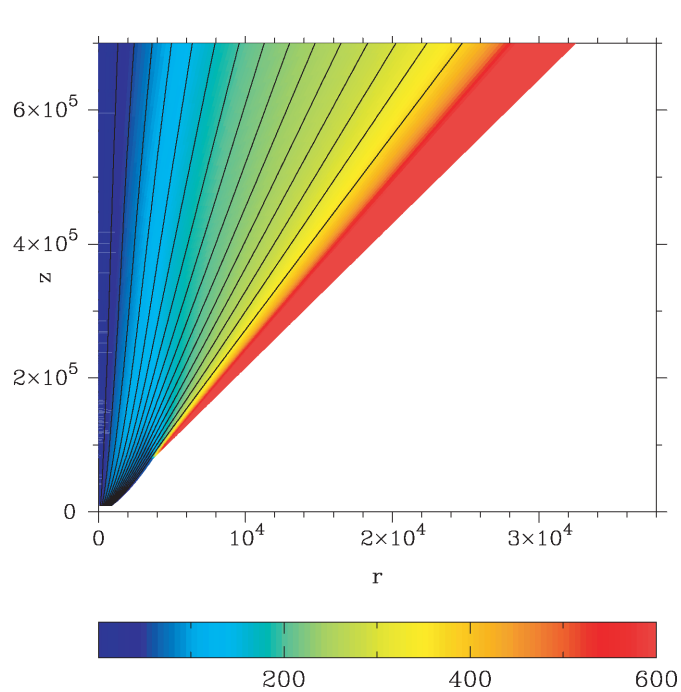


Komissarov+ 2007



- Flow near the axis is non-relativistic and self-collimated
- Then the outer part expands and accelerates
- Equipartition between Poynting and Kinetic \leftrightarrow blazar emission model

Additional conversion mechanisms



- Rarefaction acceleration
- Kink instability/RT instability
- Magnetic reconnection

Komissarov+ 2010; Porth & Komissarov 2015; Perfrey+2015

SR hydrodynamics of two-component jet

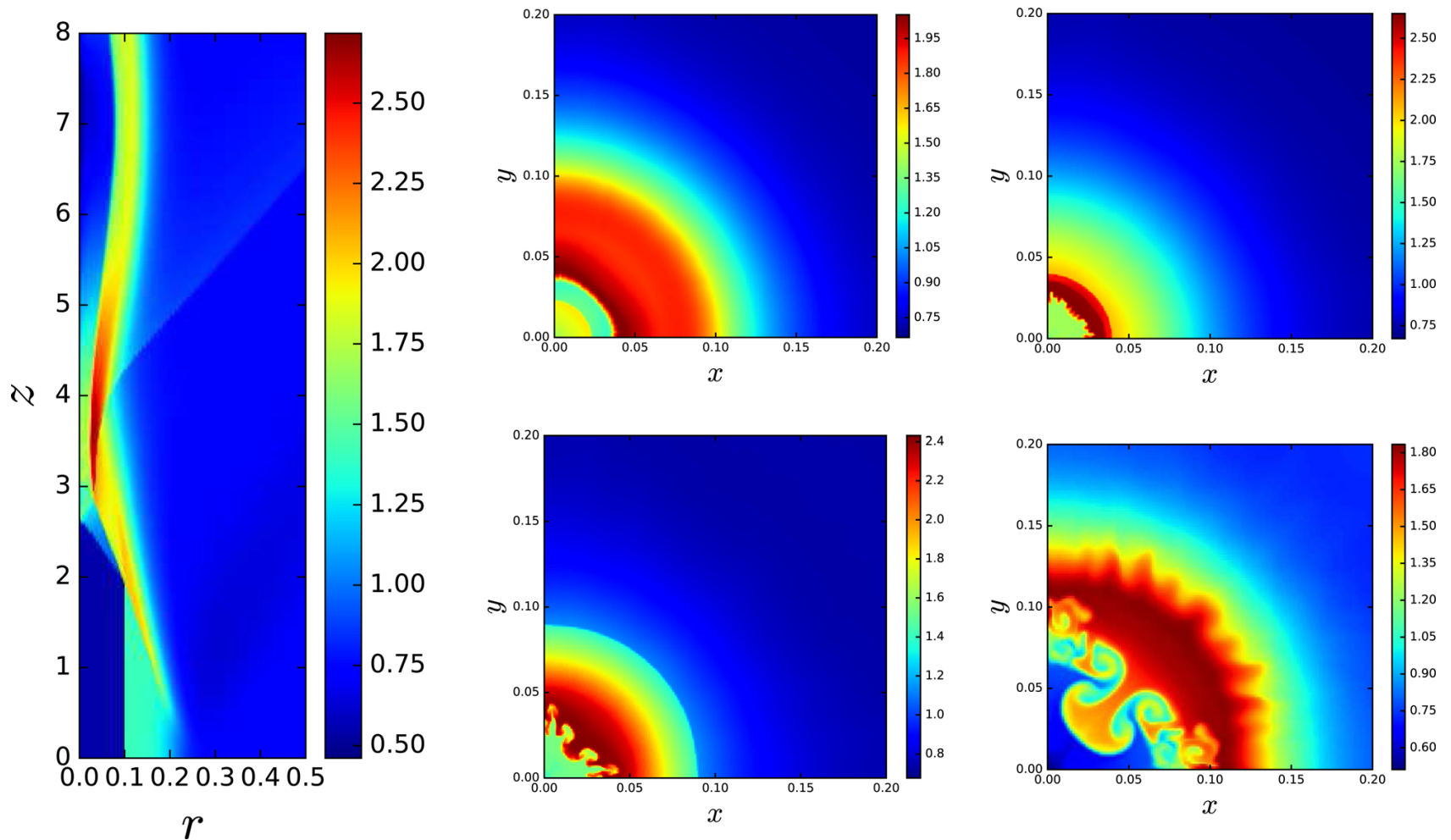
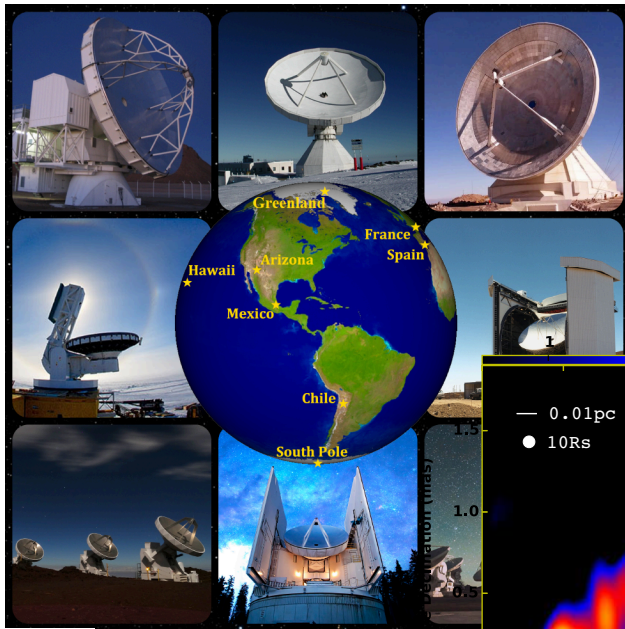


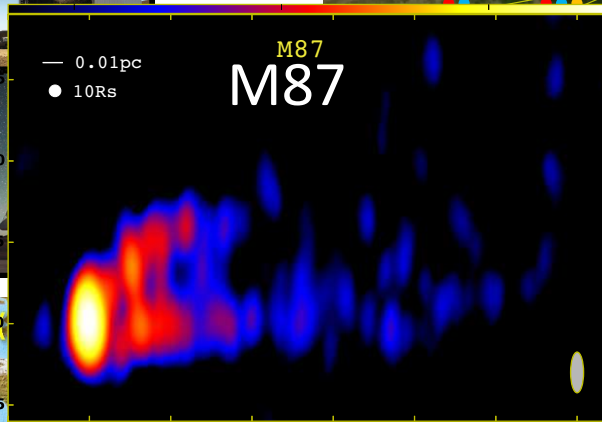
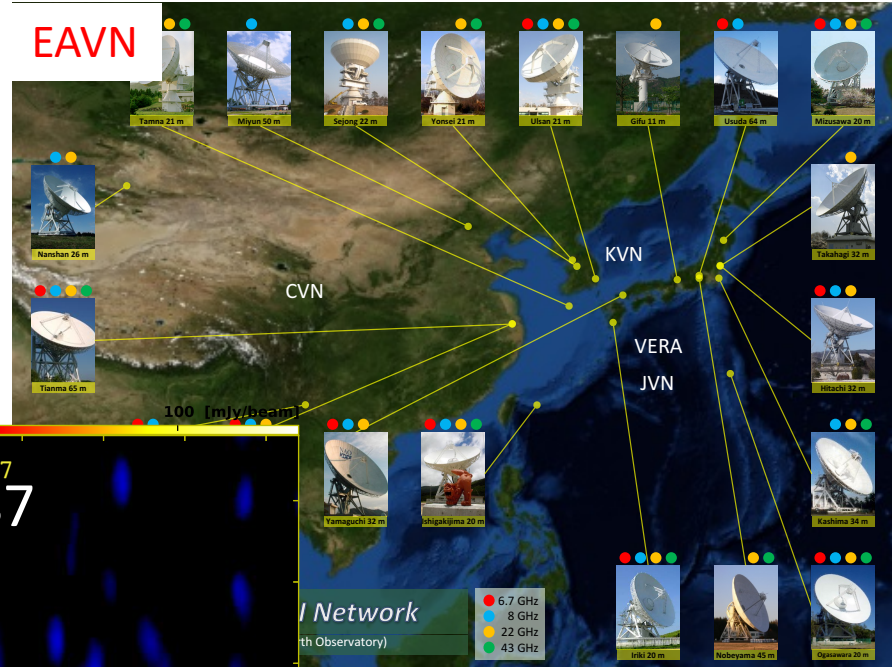
Figure 2. Left: the steady-state solution for the LSHS jet based on 1D time-dependent simulations. Right: the transverse structure of the jet with the same initial condition as the left panel at $z = 2.6$ (top-left), $z = 3.2$ (top-right), $z = 4$ (bottom-left) and $z = 7$ (bottom-right) based on 2D time-dependent simulations. The parameter shown is the effective inertia $\log(\rho h \Gamma^2)$.

VLBI

Event Horizon Telescope



EAVN

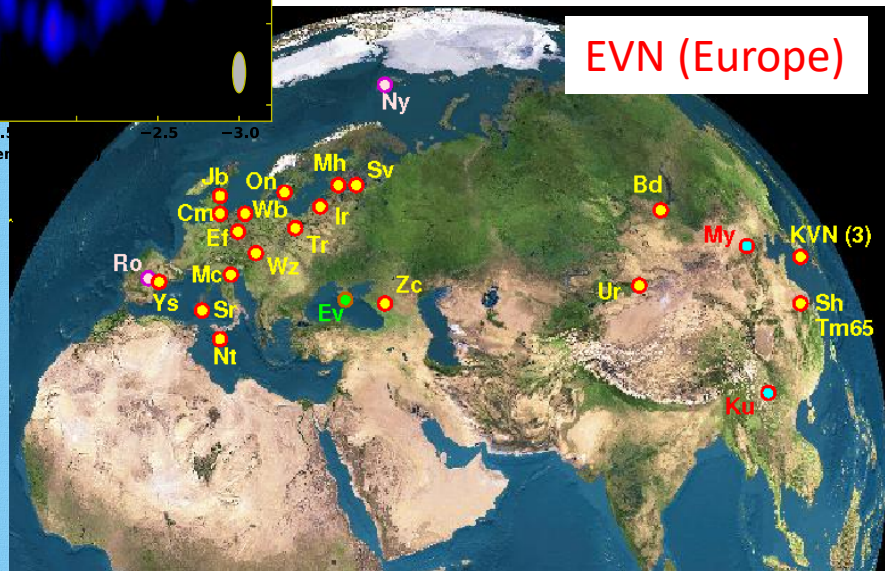


VLBA(USA)

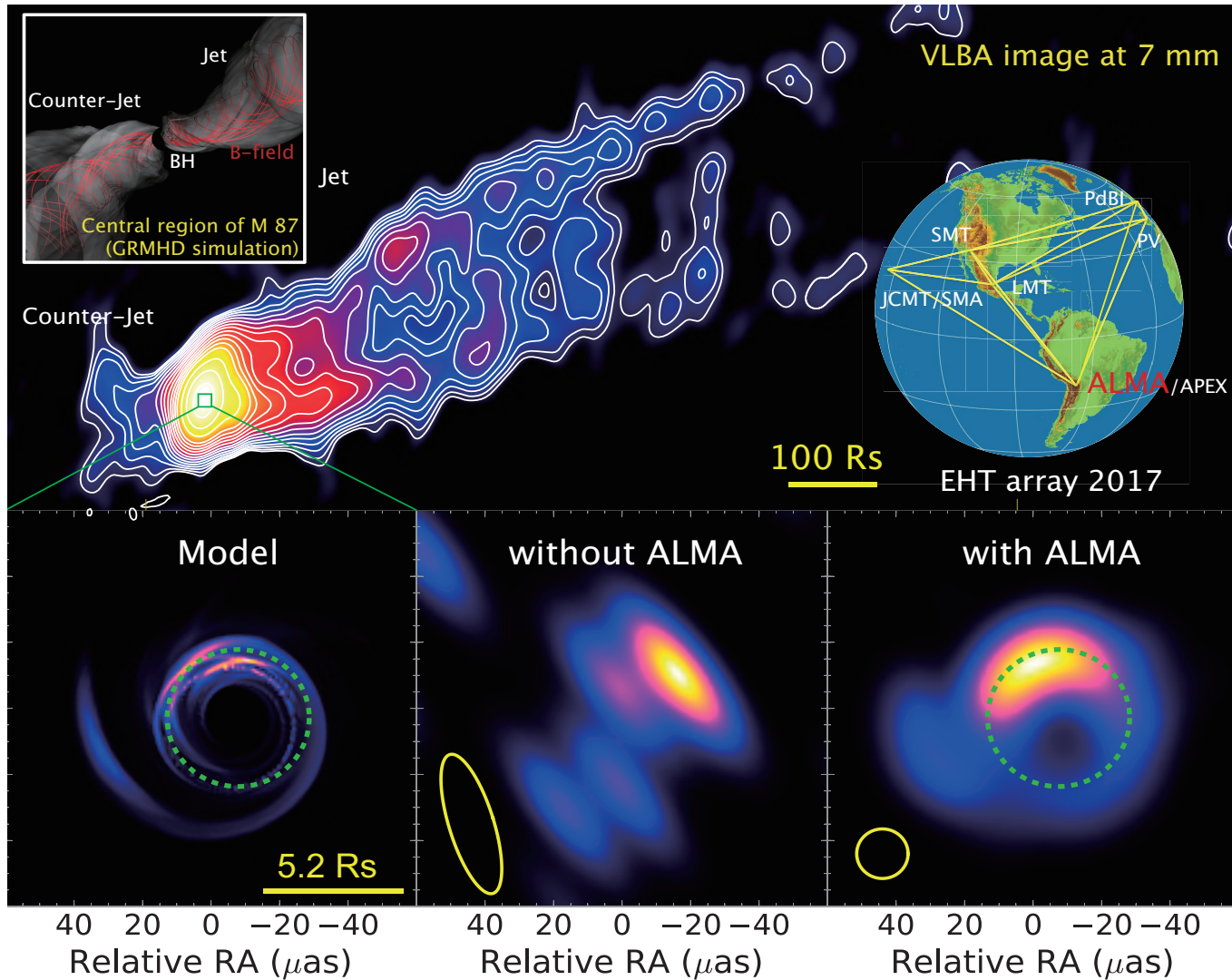
The Very Long Baseline Array



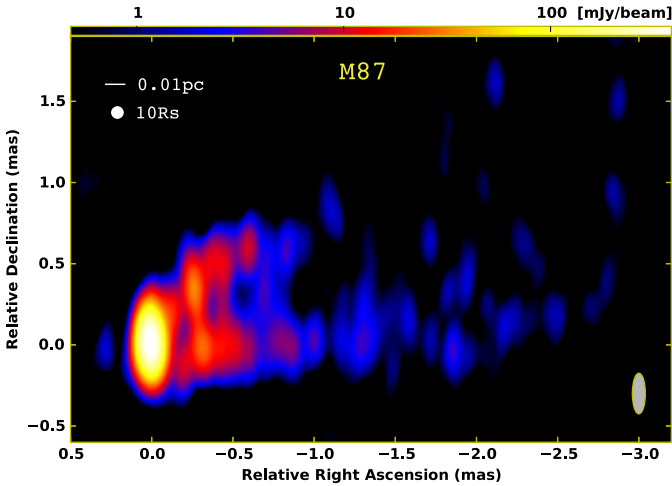
EVN (Europe)



Event Horizon Telescope

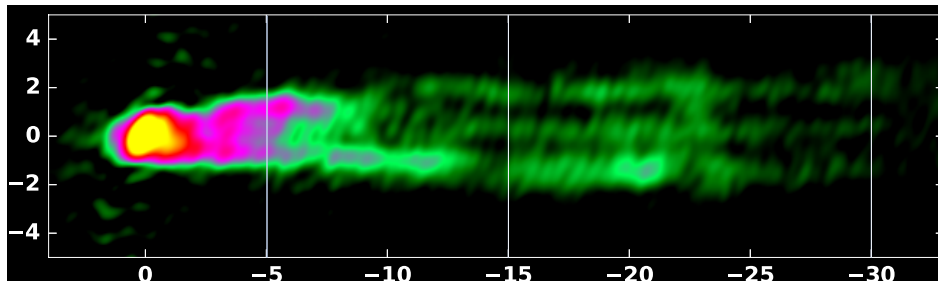
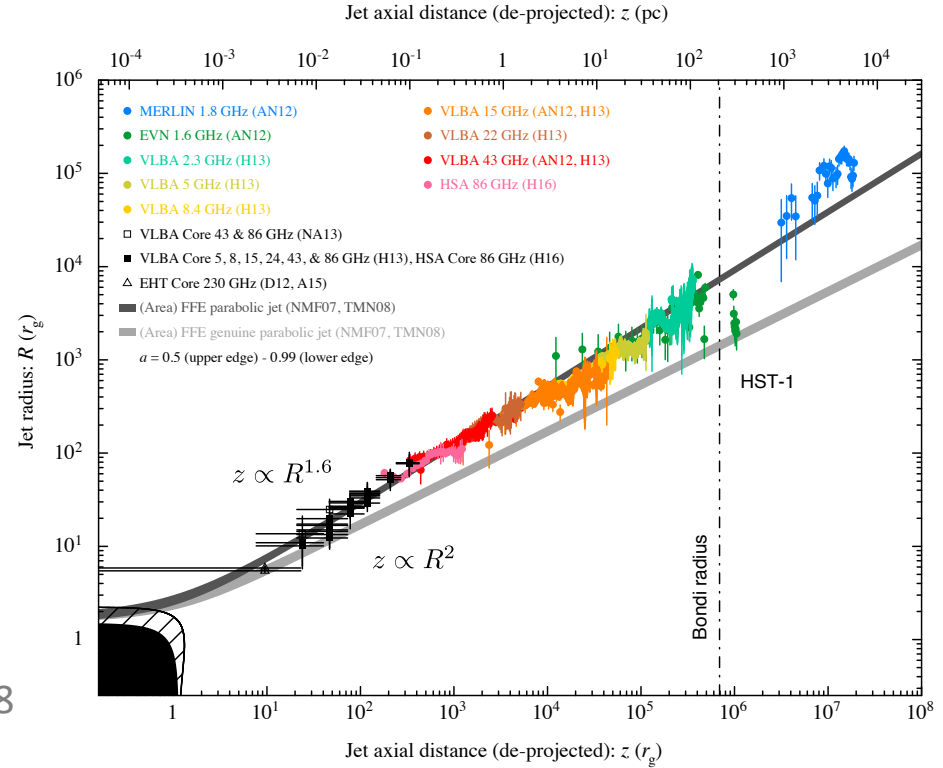


VLBI: recent progress for M87

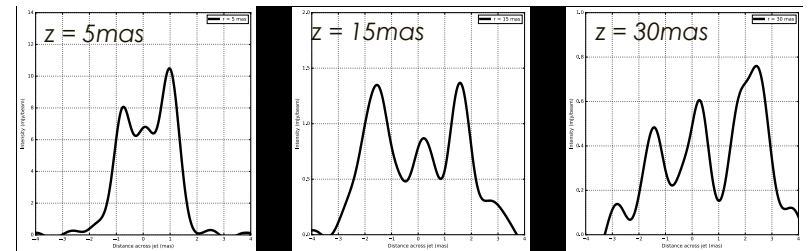


86 GHz (3.5mm); VLBA+GBT

Hada et al. 2016; 2017; Nakamura, Asada et al. 2018

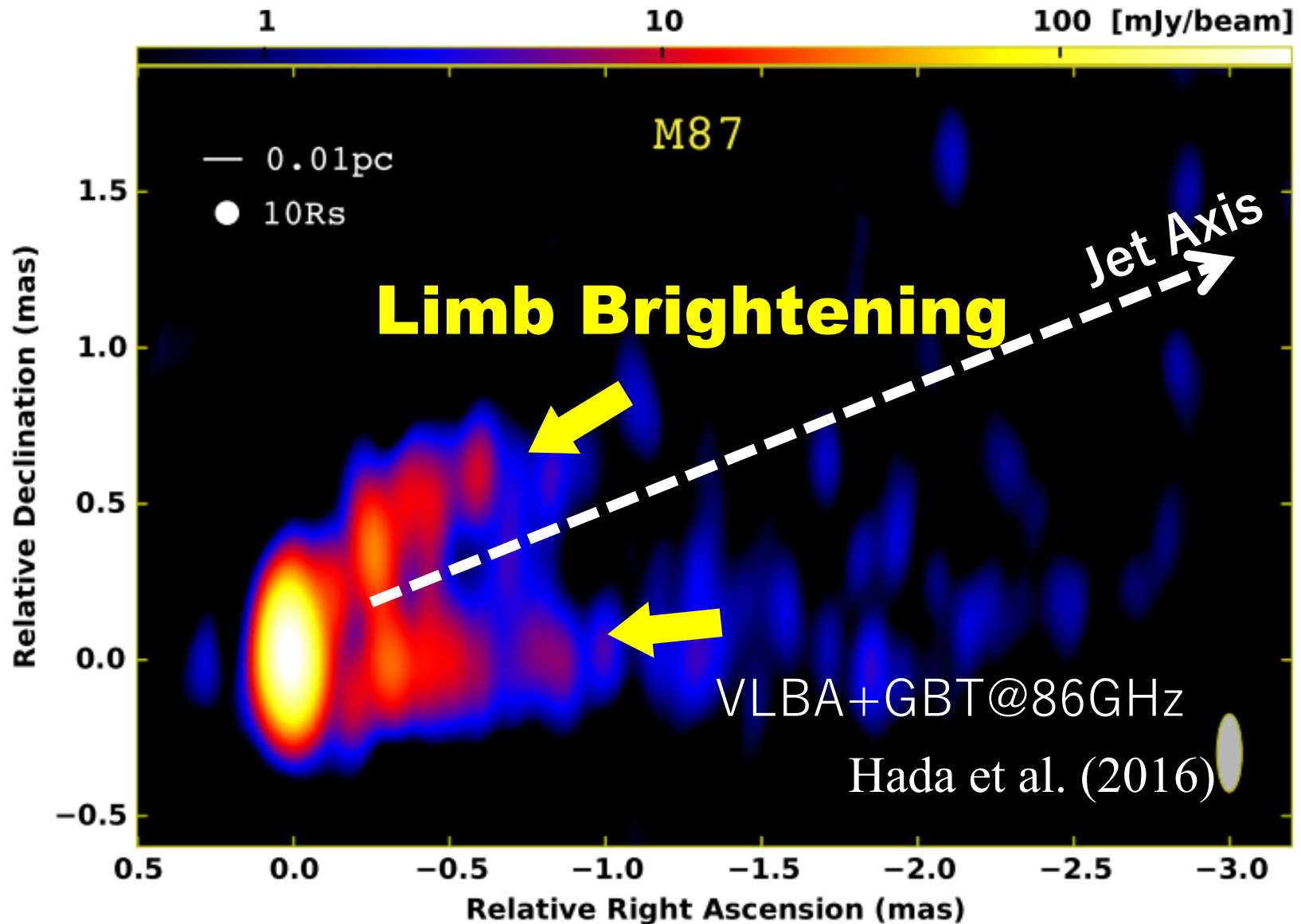


15 GHz; VLBA+VLA

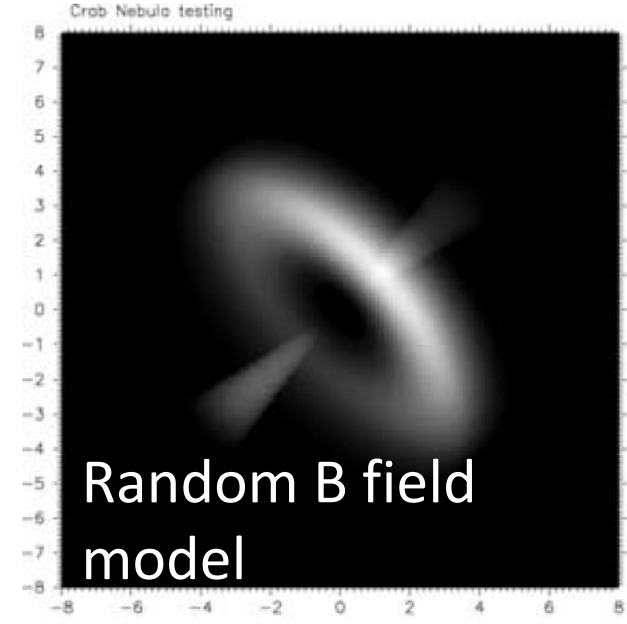
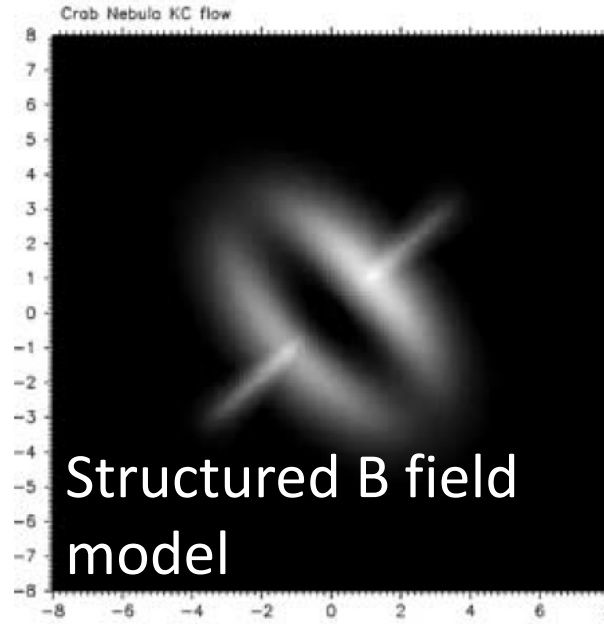
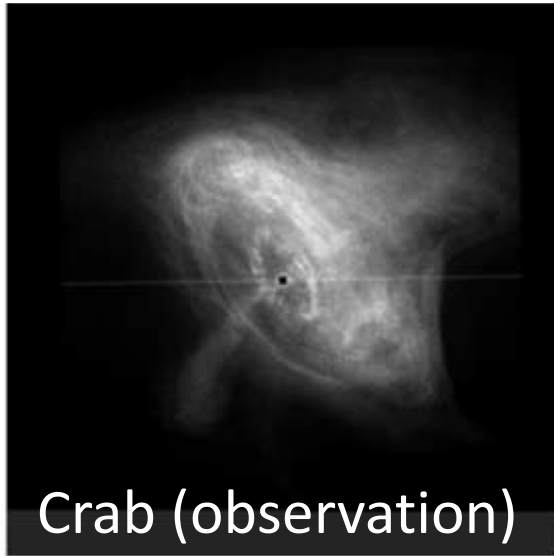


-> See Ogihara's talk

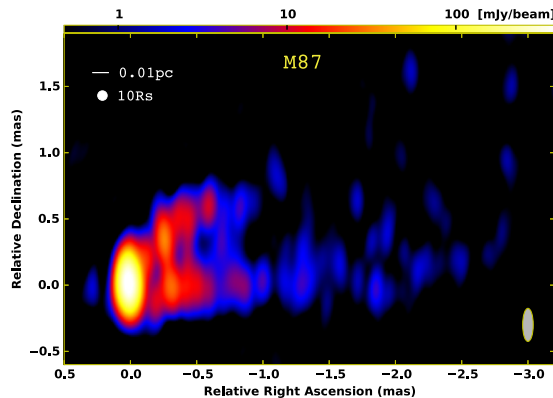
Limb-brightening



Images of relativistic outflows

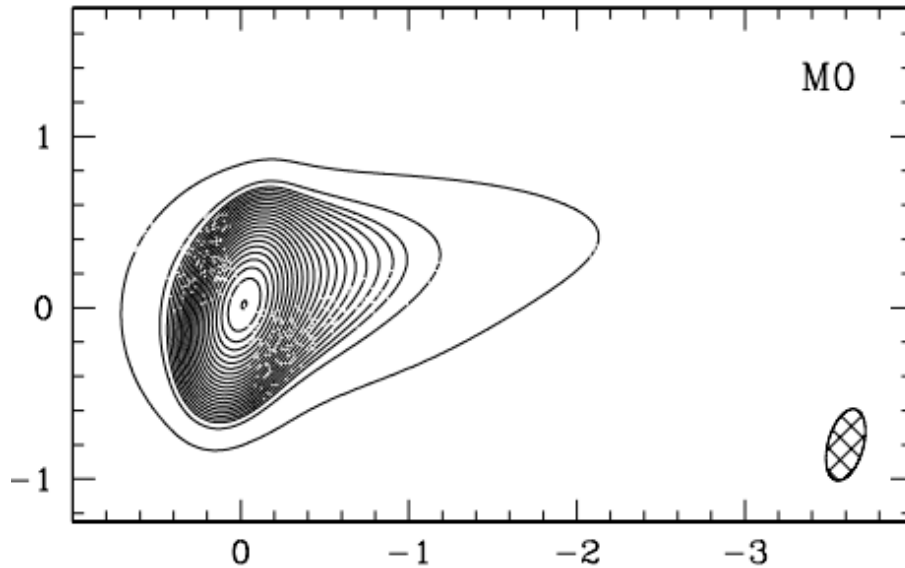


S. Shibata et al. 2003

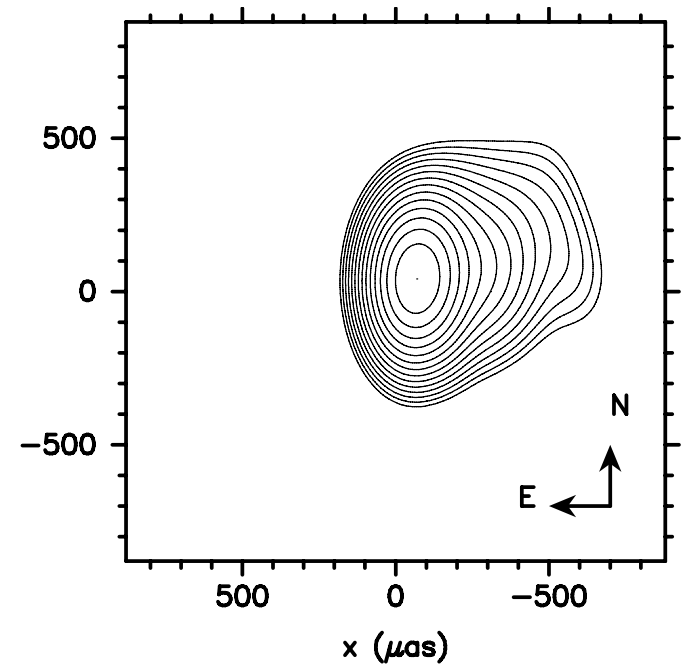


- Brightness distribution depends on n_e , B , v
- -> Observed images would constrain these quantities

Current GRMHD models



Steady axisymmetric force-free model



3D GR MHD simulation & radiative transfer

- They also show images just around BH to be compared with upcoming EHT data
- But they do not care about the limb-brightening

Steady axisymmetric force-free model

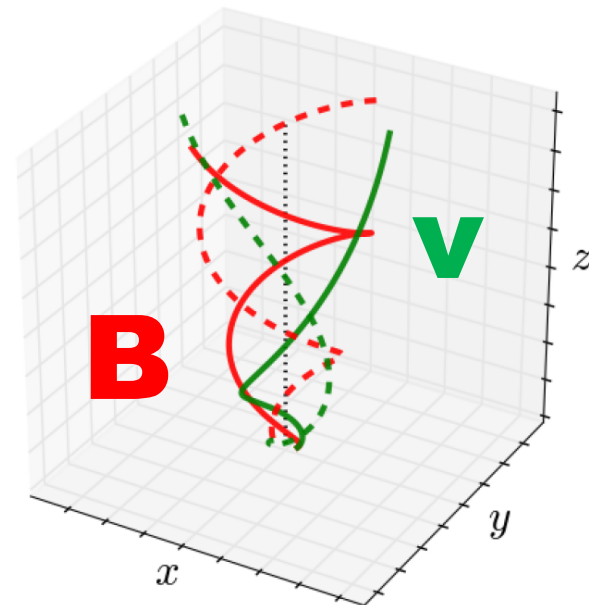
$$\Psi = Ar^\nu (1 \mp \cos \theta) \quad \text{Consistent with numerical FF simulations}$$



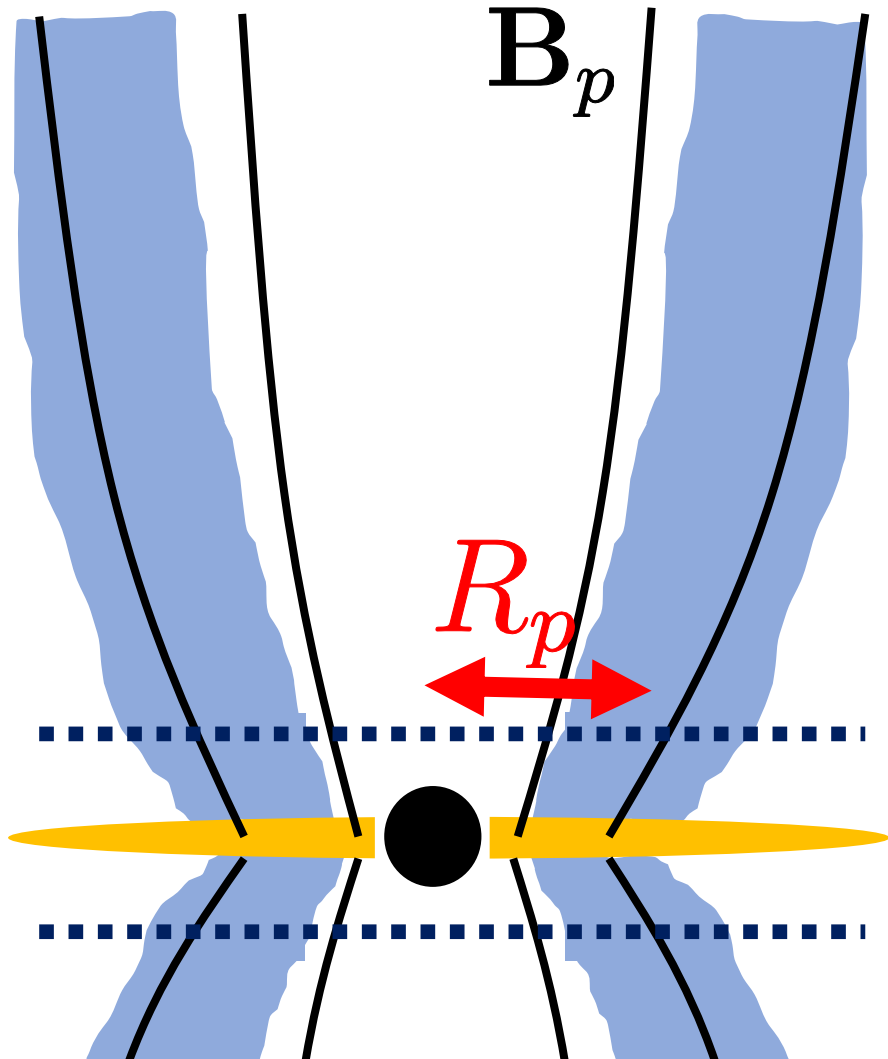
$$\mathbf{B}_p = \frac{1}{R} \nabla \Psi \times \hat{\phi}, \quad B_\phi = \mp \frac{2\Psi\Omega}{Rc}$$

$$\mathbf{E} = -\frac{1}{c} \Omega \nabla \Psi = -\frac{R\Omega}{c} \hat{\phi} \times \mathbf{B}$$

$$\mathbf{v} = \frac{\mathbf{E} \times \mathbf{B}}{B^2} c, \quad \text{Approaching MHD velocity at far zone}$$



Parametrize electron distribution



$$\nabla \cdot (n\mathbf{v}) = 0$$

$$\rightarrow \mathbf{B} \cdot \nabla \left(\frac{n}{B^2} \right) = 0$$

A constant fraction of electrons are assumed to have **power-law energy distribution**

$$n(R, \pm z_1) = n_0 \exp \left[-\frac{(R - R_p)^2}{2\Delta^2} \right]$$

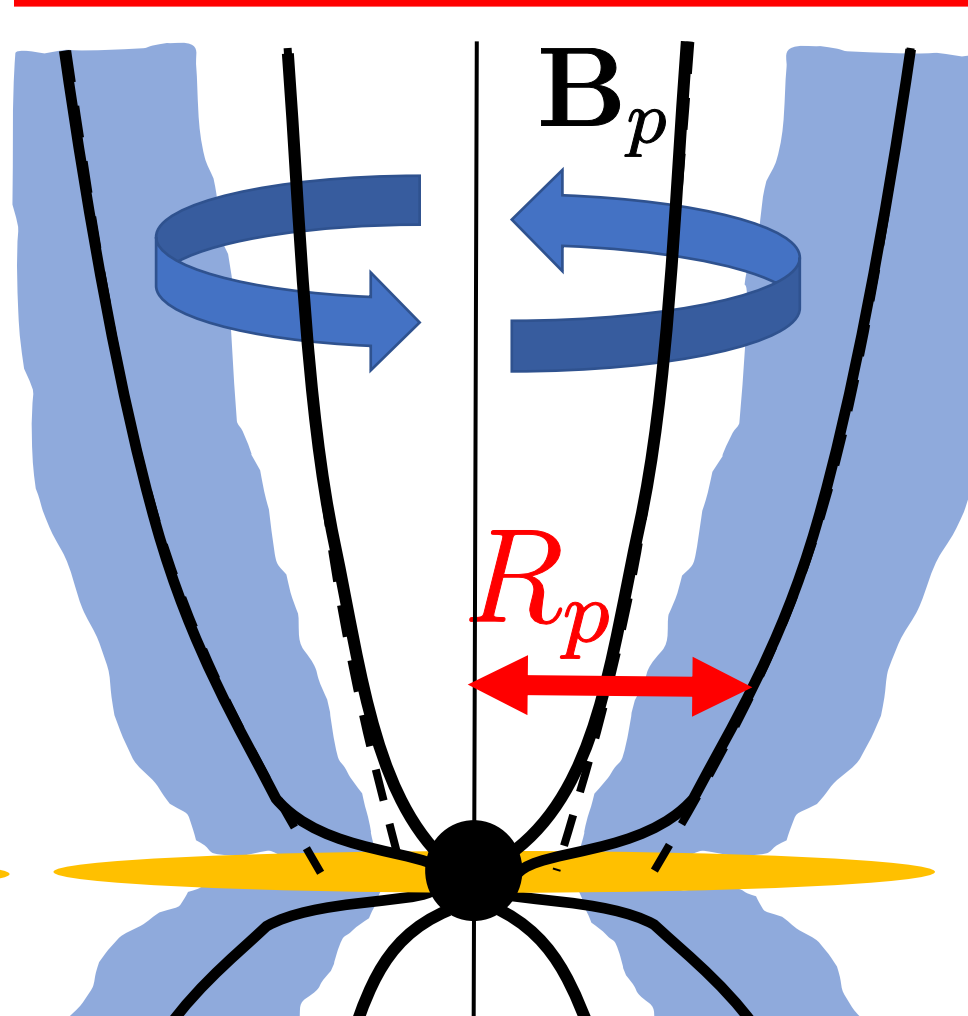
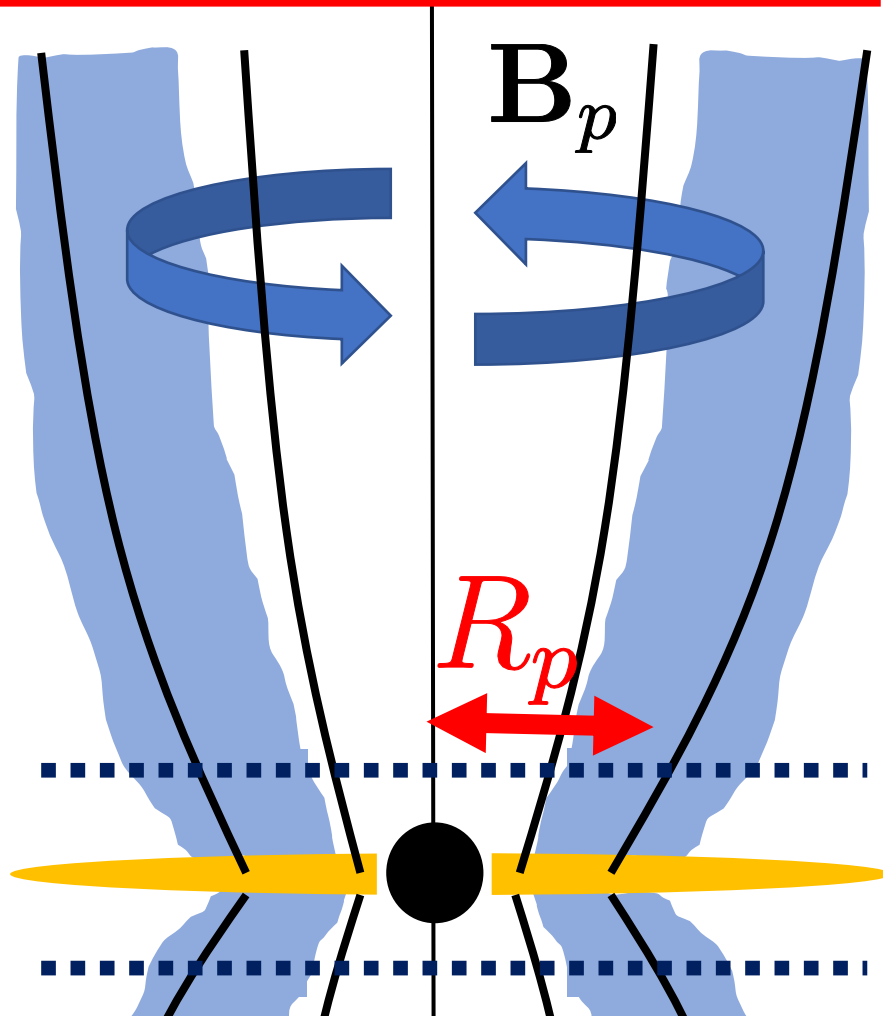
- $z_1 = \Delta = 5 r_g$: fixed
- R_p : varied

BP type: B fields threading disk

$$\Omega = \Omega_{\text{Kep}} = \sqrt{\frac{GM}{R^3}}$$

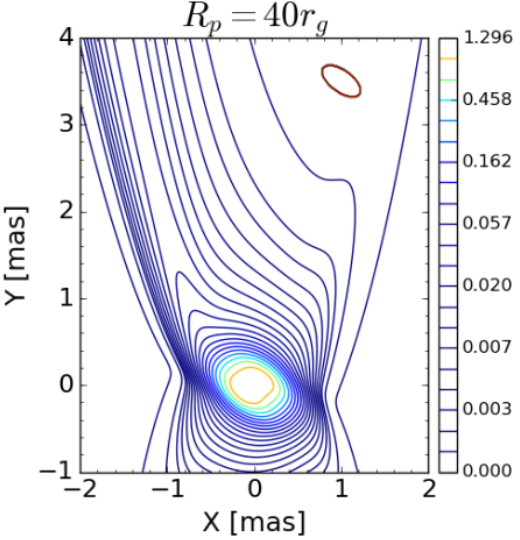
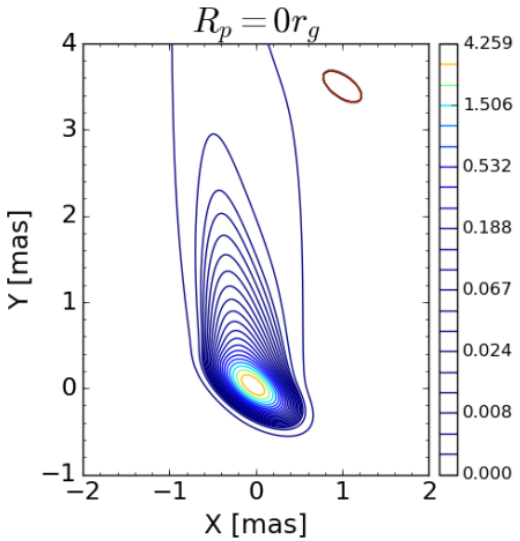
BZ type: B fields threading BH

$$\Omega = \frac{1}{2}\Omega_{\text{BH}} = \text{const.}$$

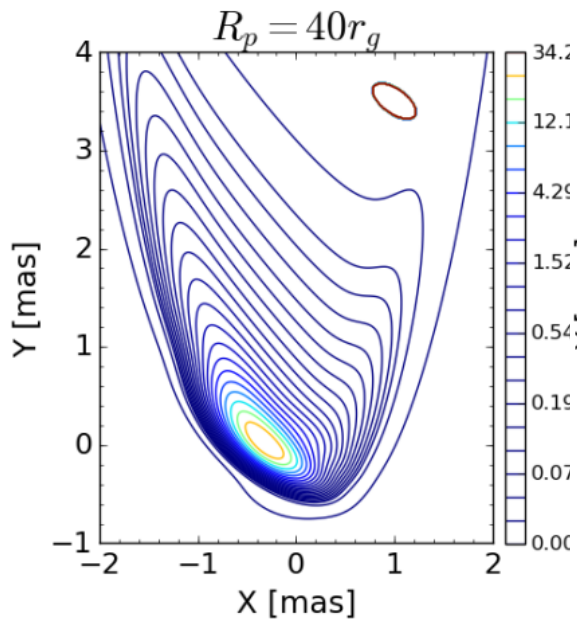
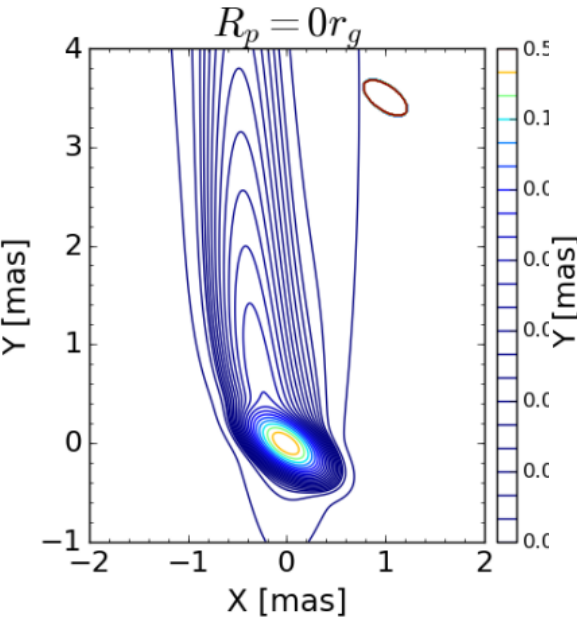


BP type: B fields threading disk

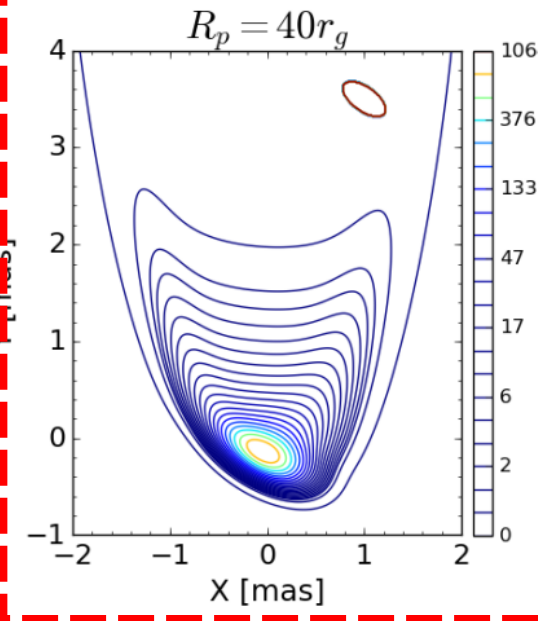
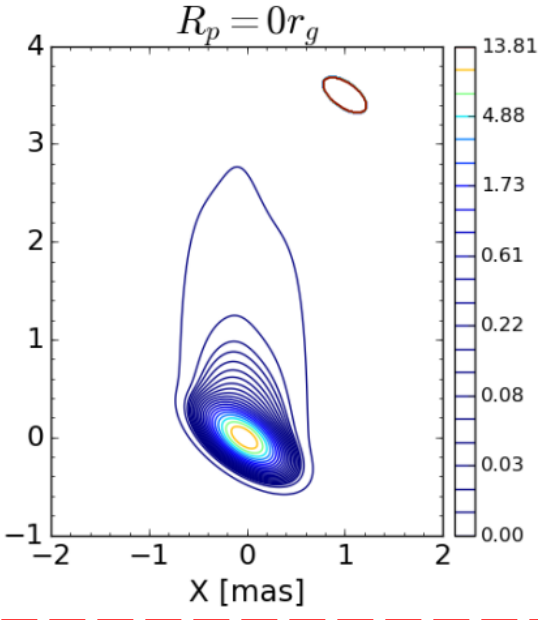
BZ type: B fields threading BH



$a = 0.1$

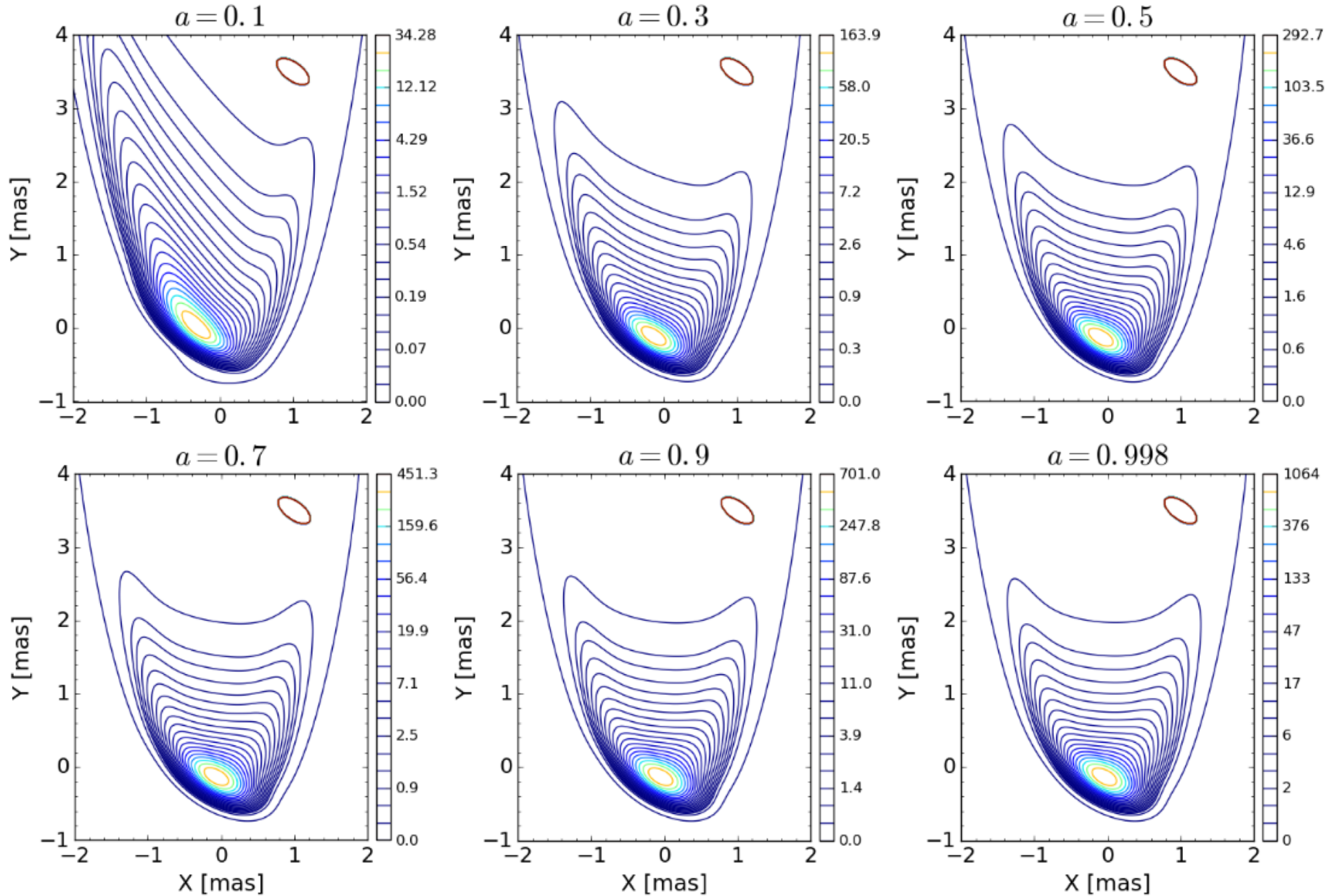


$a = 0.998$



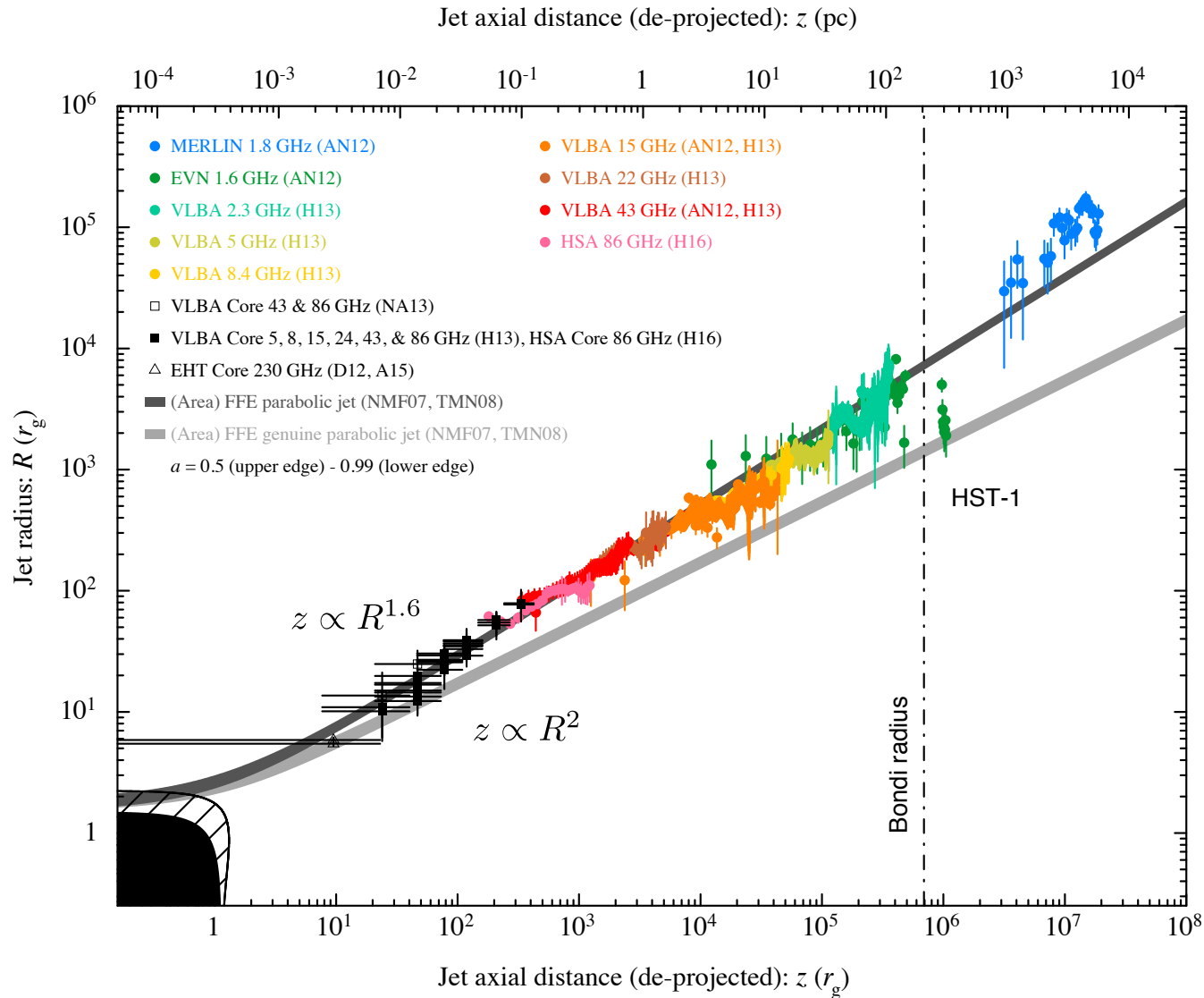
Symmetric images need high Ω (leading to low v_ϕ)

Dependence on BH spin parameter

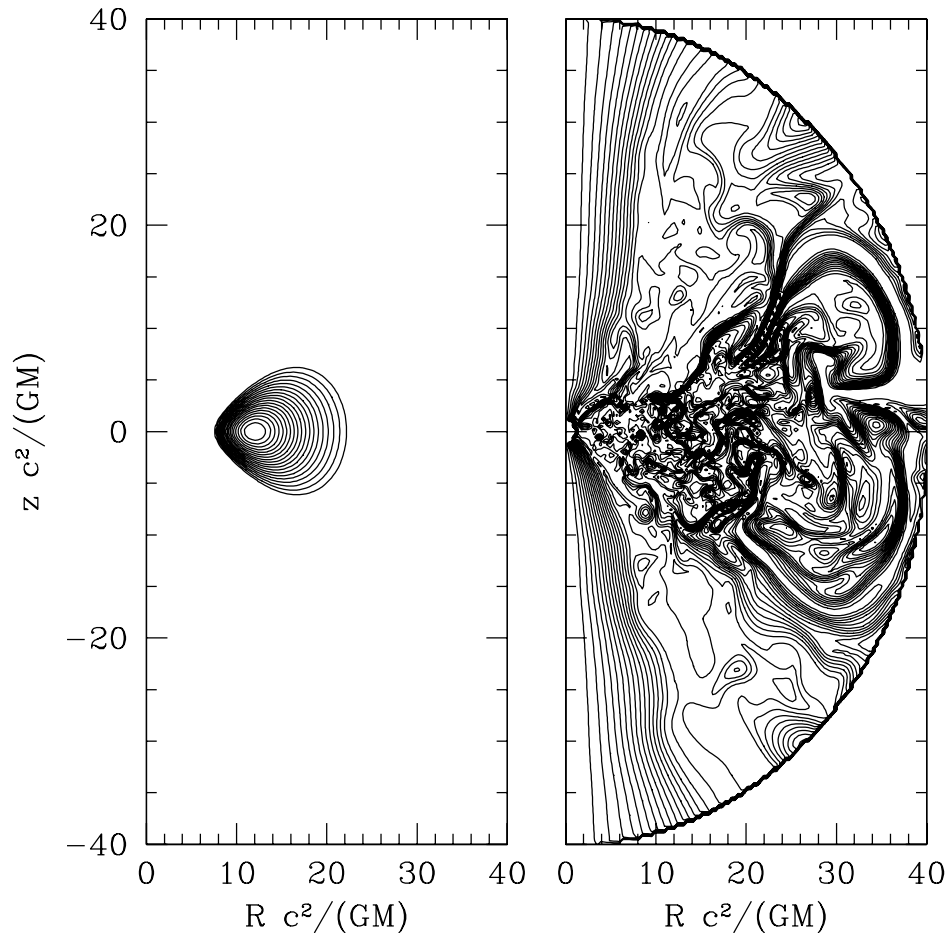


High BH spin parameter \rightarrow Symmetric image

Jet width profile



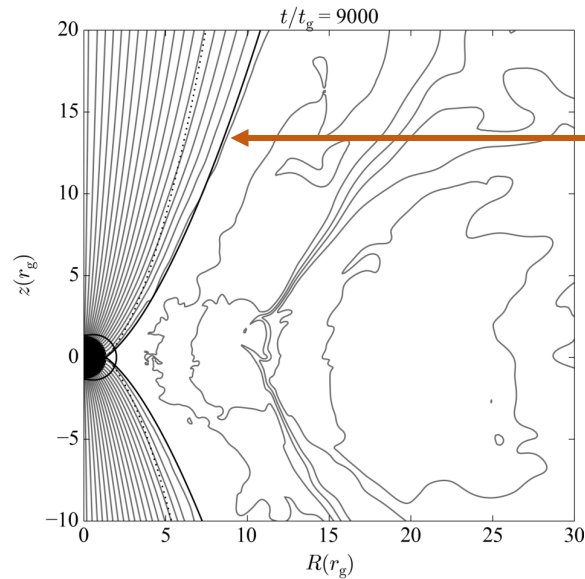
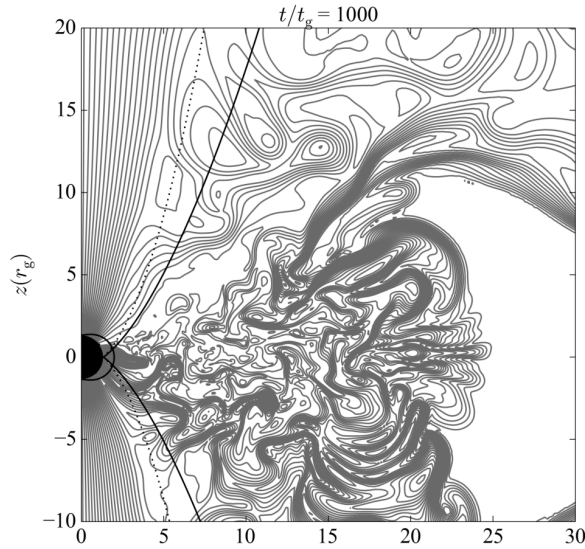
GRMHD simulations



- HARM-2D code
- Initial condition: hydrodynamically equilibrium torus
- Starting with putting poloidal B loop
- Density floor:

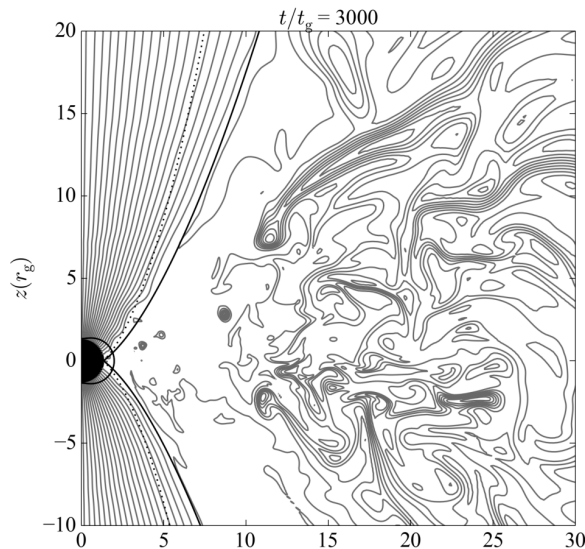
$$\rho_{\min} = 10^{-4} (r/r_{\text{in}})^{-3/2}$$

Long-term simulation

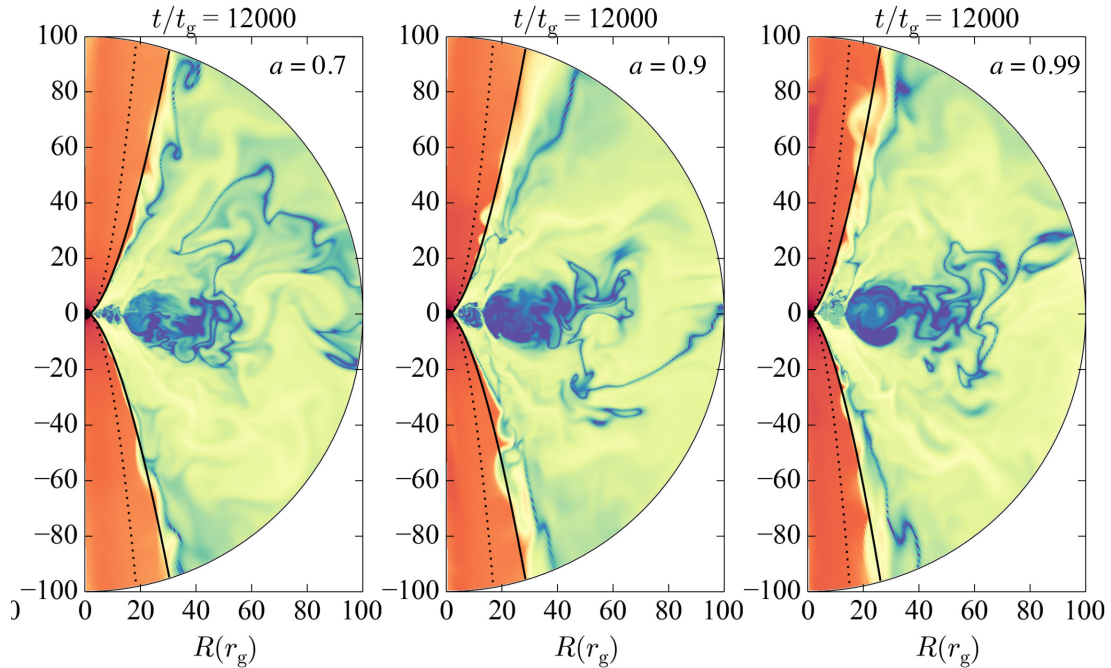


$$z \propto R^{1.6}$$
$$(\kappa = 0.75)$$

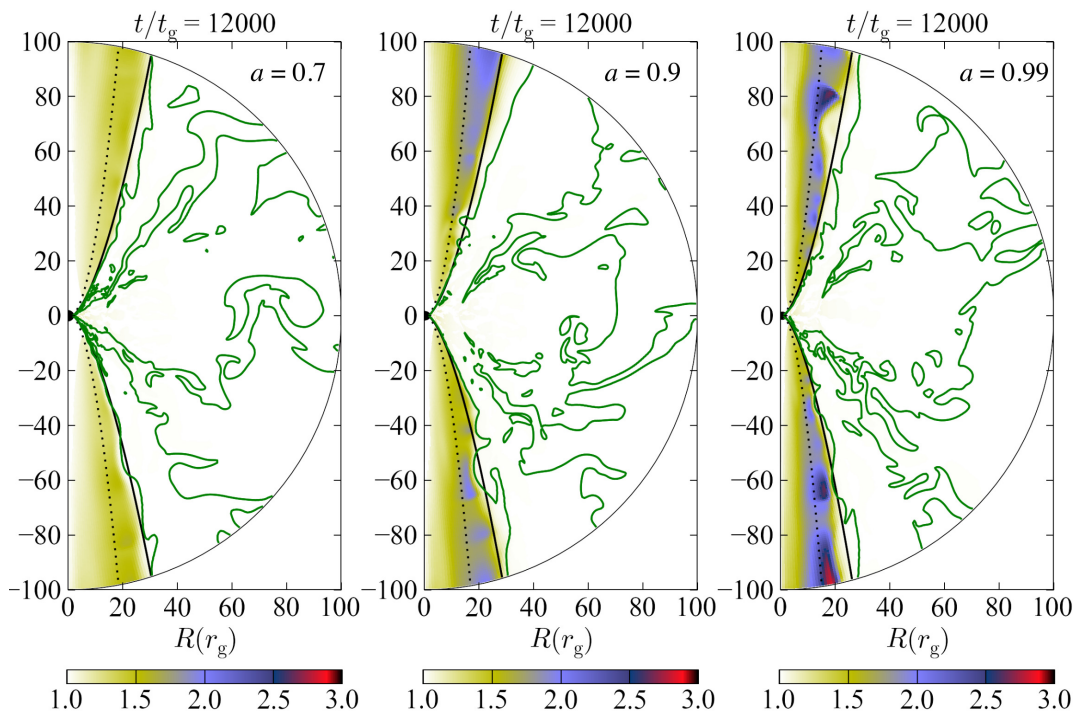
$$\Psi(r, \theta) = \left(\frac{r}{r_H} \right)^\kappa (1 - \cos \theta)$$



- All simulations so far stop at $t < 2000$
- We confirmed the steady state is reached at $t > 3000$.
- The funnel edge consistent with the jet width profile (!)



b^2 / ρ



Γ

Agreement with force-free solution

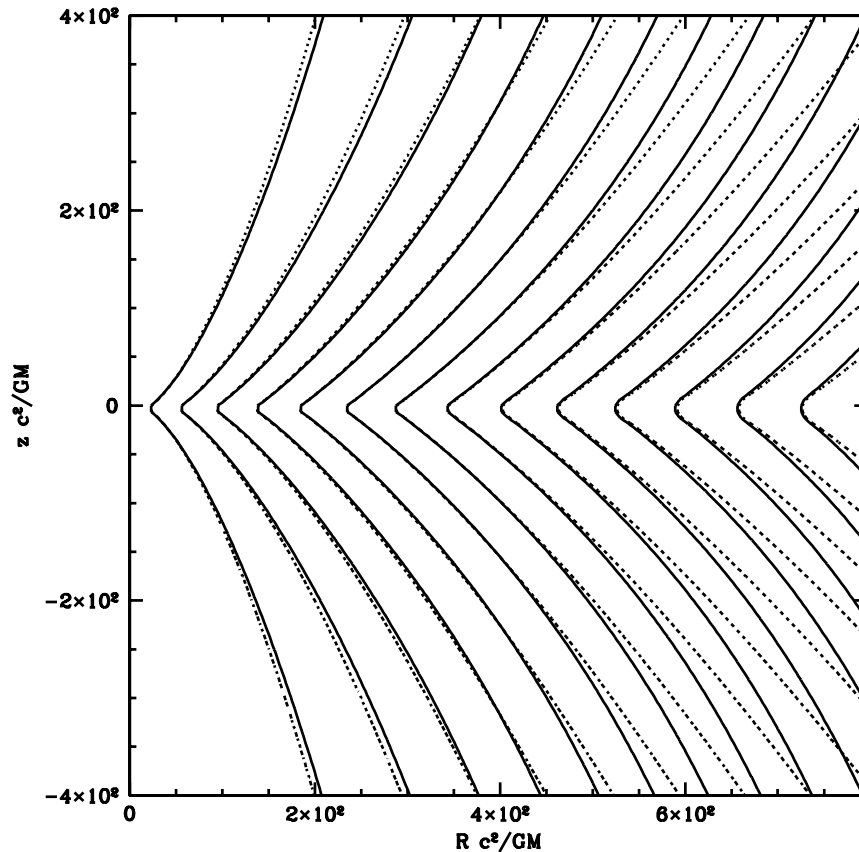
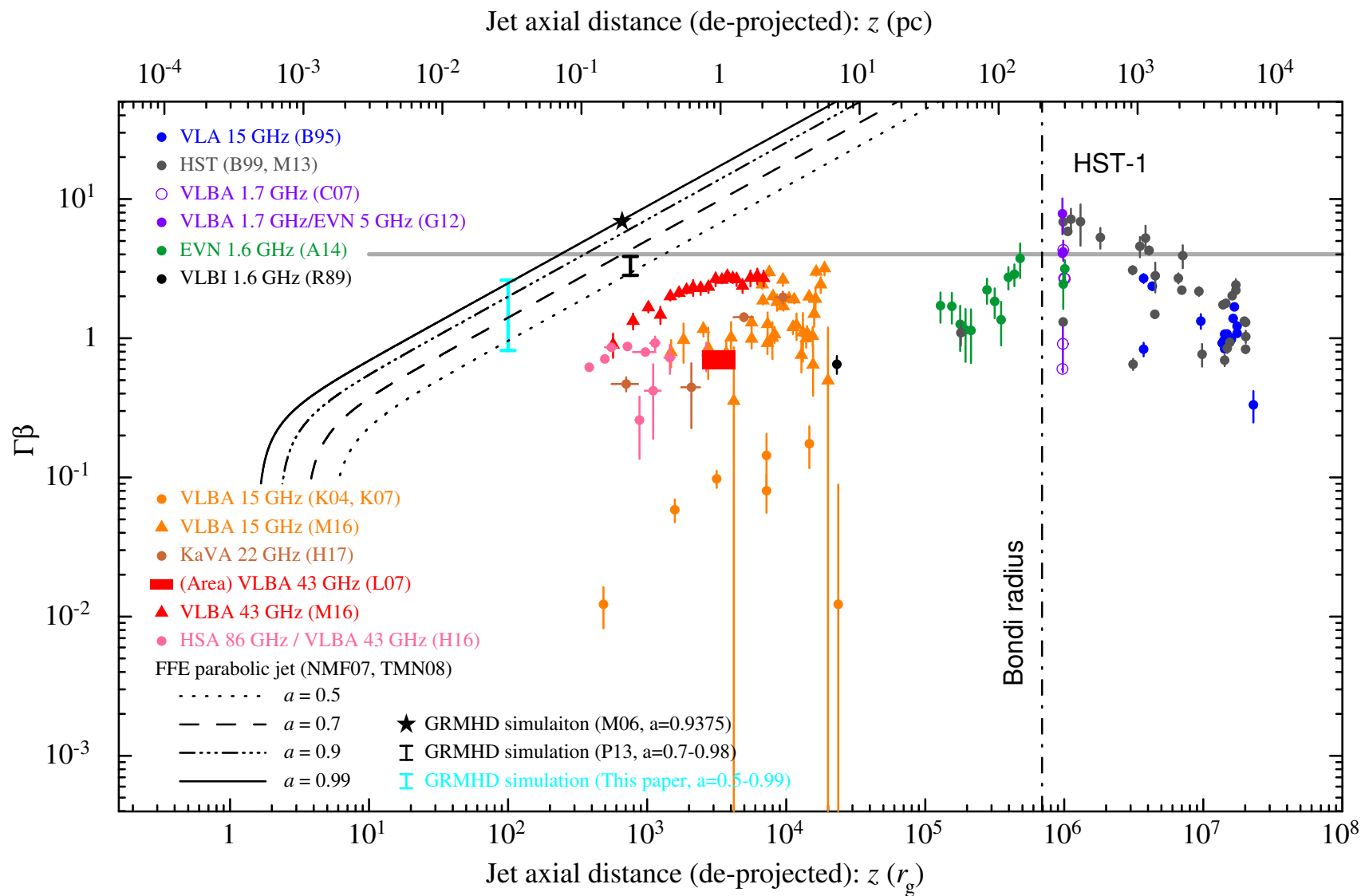


Figure 13. Field lines for the $a/M = 0.1$ GRFFE model with $\nu = 3/4$ at $t = 0$ (initial state, non-rotating solution, dotted lines) and $t = 1.2 \times 10^3 t_g$ (final converged rotating solution, solid lines). The field lines threading the black hole show mild decollimation, as in the paraboloidal case, and the field lines from the outer regions of the disc show some collimation.

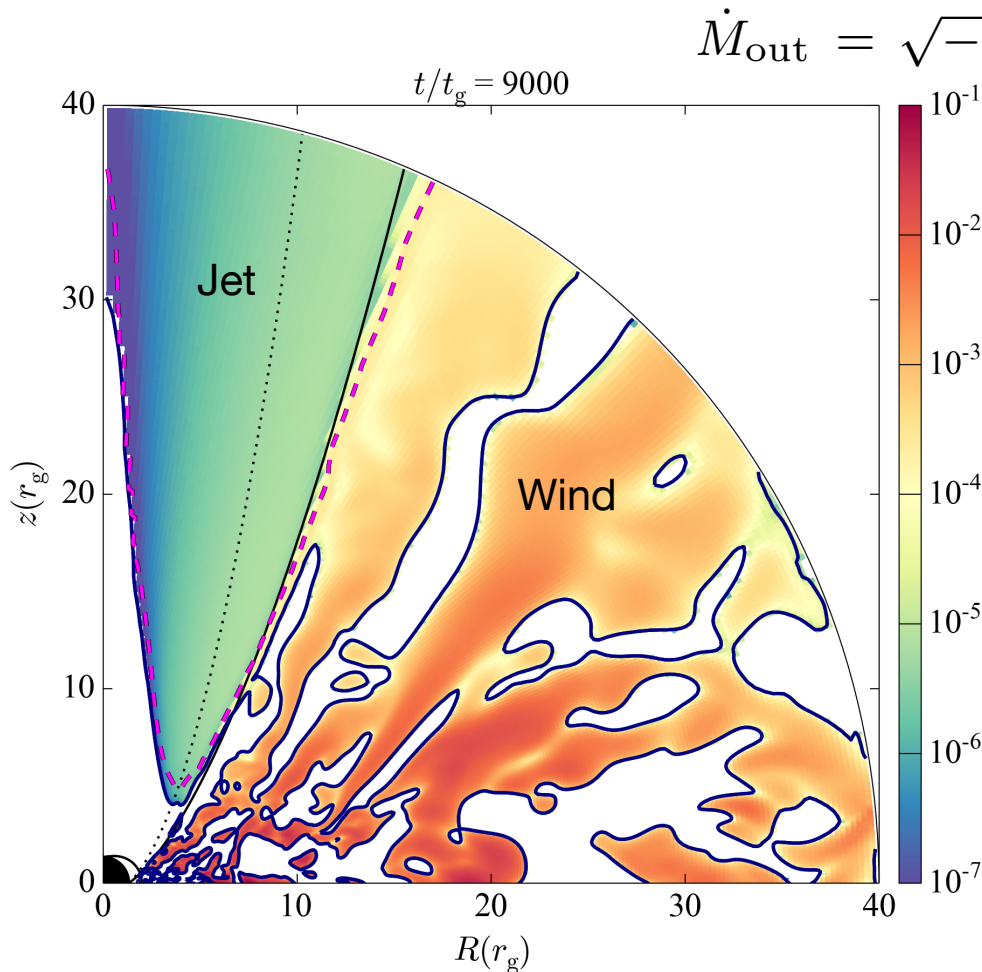
$$\Psi(r, \theta) = \left(\frac{r}{r_H} \right)^\kappa (1 - \cos \theta)$$

$$\kappa = 0.75$$

MHD velocity vs superluminal motion



Mass-loading mechanism?



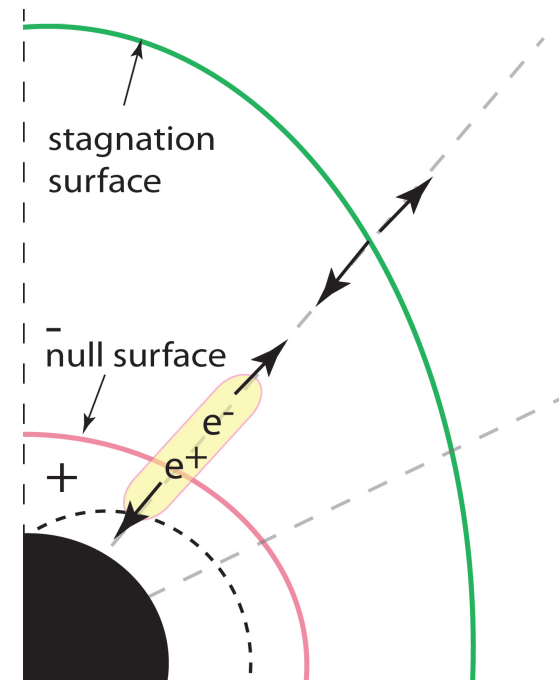
- Stagnation surface
- Rough agreement with **surface where gravity = centrifugal force**
- Particle distribution might be determined at this surface
-> related to limb-brightening?

Pair production

number density of MeV photons in the magnetosphere:

$$n_\gamma = \frac{q_{\text{ff}} 2\pi r^3 \ln(r/r_s)}{2\pi c r^2 \epsilon_\gamma} \simeq \frac{0.2 q_{\text{ff}} r^3}{c r_s^2 \epsilon_\gamma} \simeq 1.4 \times 10^{11} \dot{m}^2 M_9^{-1}$$

$$n_\pm = \sigma_{\gamma\gamma} n_\gamma^2 r_s / 3 \simeq 3 \times 10^{11} \dot{m}^4 M_9^{-1} \text{ cm}^{-3}.$$



$$n_\pm / n_{\text{GJ}} \simeq 6 \times 10^{12} \dot{m}^{7/2} M_9^{1/2}.$$

Levinson & Rieger 2011; Levinson & Segev 2017

See also Hirotani & Pu 2016; Broderick & Tchekhovskoy 2015

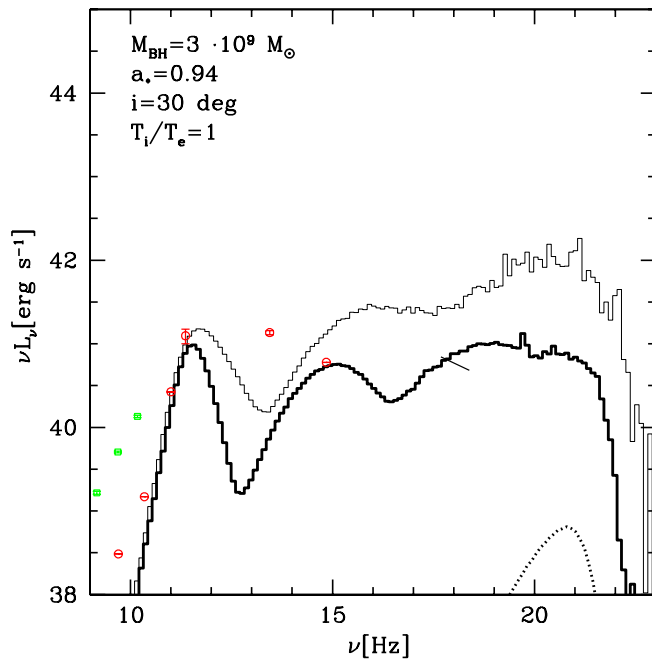


Figure 10. Model L: time-averaged spectral energy distribution. Two lines show the model with $\dot{m} = 10^{-6}$ and $T_i/T_e = 1$. \dot{m} is chosen to normalize to 1.7 Jy

- Breakdown of MHD (pair-creation gap) at null surface and stagnation surface(?)
- Dynamic kinetic physics
-> PIC simulation in BH magnetosphere

Summary

- Energy source of M87 jet is suggested to be the rotating BH by symmetry and profile of the limb-brightening image
- This should be confirmed by EHT observations
- It needs detailed modeling of mass loading, dissipation and emission